ELSEVIER

Catalysis Today 72 (2002) 101–105

CATALYSIS TODAY

www.elsevier.com/locate/cattod

# Effect of treatments on gold nanoparticles Relation between morphology, electron structure and catalytic activity in CO oxidation

L. Guczi [a,*], D. Horváth [a], Z. Pászti [b], G. Petõ [b]

[a] *Department of Surface Chemistry and Catalysis, Institute of Isotopes and Surface Chemistry, CRC, HAS Chemical Research Centre, PO Box 77, H-1525 Budapest, Hungary*

[b] *Research Institute of Technical Physics and Materials Science, PO Box 49, H-1525 Budapest, Hungary*

**Abstract**

The morphology, electron structure and catalytic activity in CO oxidation of the following samples were compared: an $Au/FeO_x/SiO_2/Si(1\,0\,0)$ model sample fabricated by pulsed laser deposition (AuPLD), an $Au/Fe_2O_3$ sample prepared by co-precipitation (AuCP) and an Au–Fe/HY (AuHY). It was established that oxygen treatment at 470 K for 1 h increases the rate of CO oxidation on AuPLD and AuCP samples as compared to subsequent hydrogen treatment at 470 K for 1 h, whereas on sample AuHY the effect is reversed. The difference cannot be ascribed to the change in particle size because the average diameter of gold particles is in the range 4–6 nm, which is only slightly modified by oxygen/hydrogen treatments. The difference among the samples cannot be ascribed to surface carbon contamination, because after oxygen treatment the amount of carbon slightly decreases and this cannot account for the activity increase.

The major difference lies in the gold/iron oxide interface, which is well developed in the case of AuPLD and AuCP, but it does not exist inside the zeolite in the AuHY sample. In the latter case, the $O_2^-$ superoxide which is responsible for the enhanced activity cannot be formed. A possible mechanism is given in this paper. 

*Keywords:* Gold/$FeO_x$ interface; Effects of oxygen and hydrogen treatments

## 1. Introduction

Since the discovery of the specific catalytic activity of gold nanoparticles [1] much data have become available but the mechanism and the various properties of supported gold are still unclear. Amongst the factors involved, the particle size, the oxidation state of gold, the choice of support and the pre-treatment conditions, e.g. oxidation/reduction, seem to be worth most consideration. As far as the particle size is concerned, the size range of the gold particles active in various catalytic reactions, such as $NO_x$ decomposition, CO oxidation, etc., is around 4–5 nm. In the early work, the type of support chosen was capable of varying its oxidation state, such as $TiO_2$, $Fe_2O_3$, $Co_3O_4$ [1], but later MgO was established as an active support which required the gold particle size to be below 1 nm [2]. There are also various findings regarding the effect of pre-treatment: in some cases oxidation increased the catalytic activity [3], in other cases hydrogen treatment gave better performance [4].

The main objective of this study was to elucidate the mechanism of the changes caused by pre-treatments,

* Corresponding author. Tel.: +361-392-2534; fax: +361-392-2307.
*E-mail address:* guczi@sunserv.kfki.hu (L. Guczi).

0920-5861/02/$ – see front matter 
PII: S0920-5861(01)00483-7

i.e. what sort of change in morphology and/or in Au particle size is responsible for the change in catalytic activity of the supported gold catalyst. We wish to summarize the features that we obtained on an $Au/FeO_x/SiO_2/Si(1\,0\,0)$ model system fabricated by pulsed laser deposition (AuPLD) (in which we used a well-defined support surface) [5], on an $Au/Fe_2O_3$ sample prepared by co-precipitation (AuCP) (when the support is granulated) [6] and on an Au–Fe/HY (AuHY) sample prepared by ion exchange of Au- and Fe-ethylene-diamine complex (when the distribution is confined by the zeolite supercage) [7].

## 2. Experimental

The $Au/FeO_x/SiO_2/Si(1\,0\,0)$ model sample was prepared by AuPLD [5] and was characterized by X-ray photoelectron spectroscopy (XPS), ultraviolet photoelectron spectroscopy (UPS) and transmission electron microscopy (TEM) in the as-prepared, oxidized and reduced states. The respective gold sizes measured by TEM were found to be 3.8, 4.1 and 5 nm. The Au 5d valence band structure was measured by means of UPS using a He(II) UV source (41 eV). The sample was sputtered by $Ar^+$ ion (1 kV and 10 mA) and the UV spectra were correlated with the surface gold concentration (in relation to the change in the gold size), similar to our experiments on cobalt nanoparticles [8]. The electron diffraction picture showed only gold lines and the iron oxide support was found to be amorphous after the first two treatments while it was partially crystallized after reduction. The Fe 2p and Au 4f binding energies were determined by XPS.

The 1 wt.% $Au/Fe_2O_3$ sample was prepared by AuCP [1] using an aqueous solution of $HAuCl_4$ and $Fe(NO_3)_3{\cdot}9H_2O$ and showed similar features, but the gold particle size was slightly higher than those measured by TEM in the AuPLD sample. XRD was used to characterize the various iron oxide phases formed after the various treatments.

The AuHY samples were prepared via ion exchange in HY ($H_{0.8}Na_{0.2}Y$, $Si/Al = 2.7$) using gold(III)-bis[ethylene-diamine]-chloride ($Au(en)_2Cl_3$) and iron(II)-[ethylene-diammonium]-sulphate tetrahydrate complexes [9]. After autoreduction of the complexes in He at 523 K, the sample was treated in $O_2$ at 573 K for 12 h to remove amine and carbon residues. Finally, the sample was treated in $H_2$ at 573 K for 1 h and considered as the as-prepared state.

The activity in CO oxidation was measured in an all glass circulation reactor using a 1:1 $CO/O_2$ ratio. The system was linked to a quadrupole Hiden mass spectrometer via a capillary leak. The initial rate of $CO_2$ formation was calculated from the slope of the $CO_2$ vs. time curves.

## 3. Results and discussion

In Table 1, the initial rates are presented for all three samples along with the rates of oxygen- and hydrogen-treated catalyst samples. The reaction temperature was different for various samples as the surface gold concentration for AuPLD and AuHY was extremely low.

It is clear that the presence of iron increased the activity in all the catalysts. The catalytic activities were measured at 520, 320 and 580 K for the AuPLD, AuCP and AuHY samples, respectively. In the presence of iron oxide irrespective of whether it is a support (AuPLD or AuCP) or promoter (AuHY), the oxidation state of gold is zero, shown by the XPS and $^{129}Xe$ NMR measurements. The Au 4f binding energies for the AuPLD, samples in the as-prepared, oxidized and reduced states were 84.2, 84.5 and 84.5 eV; for AuCP the respective values were 84.3, 83.9 and 83.8 eV. For the AuHY samples no Au 4f and Fe 2p XPS signals were obtained indicating that the species are inside the zeolite supercage. Only the $^{129}Xe$ NMR studies revealed the presence of gold in zero oxidation state in the presence of iron [7].

Table 1
The rates of $CO_2$ formation (in $\mu mol\, mg_{Au}{}^{-1}\, min^{-1}$ unit) for various samples as a function of oxygen and hydrogen treatments

| Treatments | Samples | | |
|---|---|---|---|
| | $Au/FeO_x/SiO_2/Si(1\,0\,0)$ | $Au/Fe_2O_3$ | Au–Fe/HY[a] |
| As-received | 13 | 0.1 | 0.6 |
| Oxygen-treated (470 K/1 h) | 35 | 11.7 | 0.8 |
| Hydrogen-treated (470 K/1 h) | 2 | 7.5 | 1.4 |

[a] $O_2$ and $H_2$ treatment were carried out at 620 K.

Table 2
Structures measured by TEM and XRD as well as the BEs of Fe 2p lines after various treatments

| Treatments | Samples | | | |
|---|---|---|---|---|
| | $Au/FeO_x/SiO_2/Si(1\,0\,0)$ | | $Au/Fe_2O_3$ | |
| | Fe 2p BE (eV) | Structure | Fe 2p BE (eV) | Structure |
| As-received | 710.7: FeO(OH) | Amorphous, no diffraction | 711: FeO(OH), $Fe_2O_3$ | Amorphous hematite |
| Oxygen-treated (470 K/1 h) | 711: $Fe_2O_3$ | Amorphous, no diffraction | 710.9: FeO, $Fe_2O_3$ | Amorphous hematite |
| Hydrogen-treated (470 K/1 h) | 710.4 | Crystalline maghemite-c | 710.2: $Fe_3O_4$, FeO | Crystalline maghemite-c |

The crucial point arises as to how we can rationalize the increase of activity in the CO oxidation reaction if the size and oxidation state of gold is more or less the same after the various treatments. The next step is to study the structural changes of the iron oxide support. XRD and XPS studies showed that the high activity of the AuPLD and AuCP samples was associated with amorphous iron oxide phase with Fe 2p binding energy = 711.3 eV. In Table 2, the features of iron oxide are presented for both catalyst samples after various treatments.

In the case of AuHY no iron oxide phase could be identified due to the lack of any XRD and XPS signal. The $FeO_x$ support contains $Fe_2O_3$ in hematite phase, FeO and FeO(OH) species. The electron diffraction pattern of this sample revealed the presence of goethite, which is the orthorhombic form of the FeO(OH). After reducing the sample the maghemite-c phase appeared; furthermore, there is a significant decrease in activity.

In conclusion, it was established that in developing the catalytic activity the gold should be metallic and the support should be in an amorphous state with high binding energy and an interface around the gold and iron oxide support developed: this perimeter is responsible for the activity.

Although both parameters mentioned, i.e. the oxidation state/particle size of gold as well as the iron oxide, are prerequisite to having an active gold/iron oxide sample, it is not sufficient to explain the enhanced activity during oxidation. One may suggest that after oxidation the surface carbon might have been removed and the active site concentration thereby increased. This is, however, not the case because the decrease of surface carbon from 18 to 8% does not account for the activity increase. Even after oxidation the amount of surface gold measured by XPS slightly decreases, e.g. on the AuPLD sample the Au in the as-prepared and oxidized states are $7.9 \times 10^{-4}$ and $6.3 \times 10^{-4}$ mg.

In order to tackle this problem, we have to consider the oxygen species measured by XPS for the oxygen 1s BE shown in Fig. 1. For the AuCP sample in the as-prepared state there are two lines at 530.3 and 533.5 eV being characteristic of $Fe_2O_3$ and $H_2O$, respectively. After oxidation, lines can be

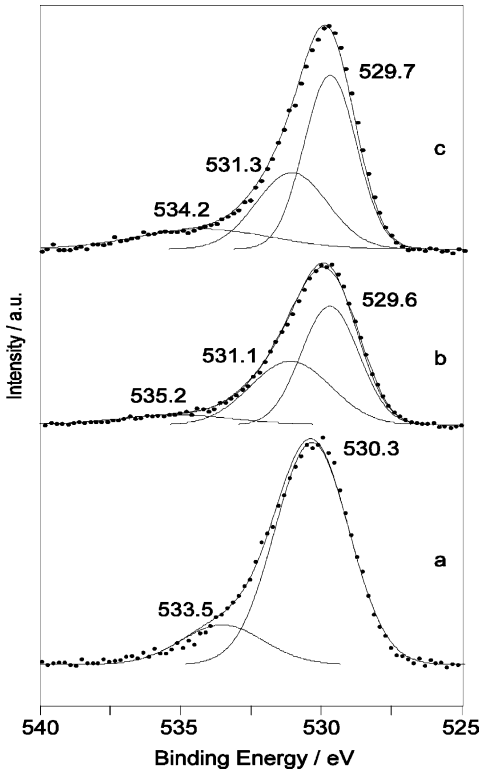


Fig. 1. O 1s BE for AuCP sample in as-prepared (a), oxidized (b) and reduced (c) states.

found at 529.6 eV (FeO), 531.1 eV (OH group) and at 535.2 eV which may be assigned to $O_2^-$ species. Similar assignments are valid for the AuPLD sample except for the line measured at high binding energy which is possibly due to low intensity as the surface area of the model catalyst is very small.

Now, we are in the position to try to rationalize why the oxidized is more active than the fresh or reduced state, except for the AuHY sample. Before we define the scenario, we have to take into consideration some additional experimental findings. Firstly, the effect observed is not primarily associated with the change of the gold particle size; secondly, without gold the oxidative treatment does not change the activity of the support, and thirdly, the *heat treatment alone* (carried out in helium) *does not affect the catalytic activity*. That is, after treatment in oxygen a change must take place at the perimeter of the gold/support interface.

We assume that at the perimeter, an oxygen vacancy is generated according to the following equations:

$$4FeO(OH) \rightarrow 4FeO + 2H_2O_{(g)} + O_{2(g)} \quad (1)$$

$$Fe^{2+} + O_{2(g)} \leftrightarrow Fe^{3+} + O_{2(s)}{}^- \quad (2)$$

At the vacancy, molecular oxygen can adsorbed and this takes one electron from the $Fe^{2+}$ species to form $O_2^-$ entities. There are several pieces of evidence to support the existence of this species [10–14]. Among them, we mention the results of Iwasawa's work using labelled oxygen and $Au/Al_2O_3$ doped by $MnO_x$. Also the oxygen species we measured by XPS, mentioned previously, points the presence of the oxygen species adsorbed at an oxygen vacancy.

The mechanism is depicted by Scheme 1 in which the change of the support characteristics at the interface plays a decisive role. Accordingly, once the FeO in amorphous form is produced (during oxygen treatment at higher temperature associated with the liberation of water) negatively charged molecular oxygen is adsorbed on the vacancy. The partial negative charge helps CO chemisorption at the gold/support interface and the oxidation of CO occurs most probably via a Langmuir–Hinselwood mechanism. We first put forward this idea [6] and recently it has been strongly supported by other authors [15].

The discrepancy that we observed between the effect of treatments carried out on AuPLD or AuCP, and on AuHY, is most likely attributed to the fact that in the AuHY sample one cannot find any well-developed iron oxide phase. Although a mixture of $Fe^{2+}$ and $Fe^{3+}$ ions may exist, but *a gold/iron oxide interface does not exist*. Earlier studies on Pt–Co/NaY system showed [16] that under gentle oxidation, the Pt particles remain in the supercage whereas the cobalt ions migrate into the smaller (sodalite and hexagonal) cages. This is most probably the case also for the Au–Fe/HY system. As we mentioned earlier, XPS does not give either Au 4f or Fe 2p signals. Only gold particles can be seen by TEM, indicating somewhat larger particles in the presence of iron. If an $FeO_x$ species existed in large enough quantity inside the zeolite cages, we would be able to see it by XRD. On the effect of hydrogen treatment, we suggest a back-migration of iron species from the smaller cages to the supercages of HY that afterwards form a degenerated type of interface accelerating thereby the rate of CO oxidation.

## 4. Conclusions

The gold/iron oxide interface along the perimeter of the gold particle and the resulting changes in morphology and electron structure are responsible for the catalytic activity in CO oxidation to $CO_2$.

A well-developed interface formed in the AuPLD and AuCP catalysts, but not for AuHY. Treatment in

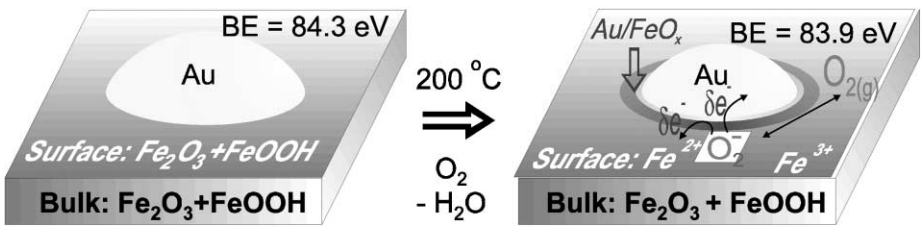


Scheme 1.

oxygen resulted in a vacancy in the lattice which accommodated a negatively charged oxygen molecule. The partial electron charge flow from the $O_2^-$ to the gold particles promoted the CO adsorption (which is normally weak) and thereby the reactivity of CO towards the oxygen to form $CO_2$ was enhanced. On the other hand, in AuHY no such interface was developed, only after hydrogen treatment when the iron species re-migrated to the supercage, increasing the activity for $CO_2$ formation.

## Acknowledgements

The authors are indebted to COST D15 projects (Grant Nos. D15/0005/99 and D15/0016/00) for partial support and to the National Science and Research Fund (OTKA Grant No. T-034520) for financial support.

## References

[1] M. Haruta, N. Yamada, T. Kobayashi, S. Iijima, J. Catal. 115 (1989) 301.
[2] D.A. Cunningham, W. Vogel, H. Kageyama, S. Tsubota, M. Haruta, J. Catal. 177 (1998) 1.
[3] N.M. Gupta, A.K. Tripathi, J. Catal. 187 (1999) 343.
[4] Y.-S. Su, M.-Y. Lee, A.D. Lin, Catal. Lett. 57 (1999) 49.
[5] L. Guczi, D. Horváth, Z. Pászti, L. Tóth, Z.E. Horváth, A. Karacs, G. Petõ, J. Phys. Chem. B 104 (2000) 3183.
[6] D. Horváth, L. Tóth, L. Guczi, Catal. Lett. 67 (2000) 117.
[7] D. Horváth, M. Polisset-Thofin, J. Fraissard, L. Guczi, Solid State Ionics, in press.
[8] G. Petõ, G. Molnár, G. Bogdányi, L. Guczi, Catal. Lett. 26 (1994) 383.
[9] D. Guillemot, V.Yu. Borovkov, V.B. Kazansky, M. Polisset-Thofin, J. Fraissard, J. Chem. Soc., Faraday Trans. 93 (1997) 3587.
[10] A. Bielanski, J. Haber, Oxygen in Catalysis, Marcel Dekker, New York, 1991.
[11] H. Liu, A.I. Kozlov, A.P. Kozlova, T. Shido, K. Asakura, Y. Iwasawa, J. Catal. 185 (1999) 252.
[12] H. Liu, A.I. Kozlov, A.P. Kozlova, T. Shido, K. Asakura, Y. Iwasawa, Phys. Chem. Chem. Phys. 1 (1999) 2852.
[13] R.J.H. Griesel, B.E. Nieuwenhuys, J. Catal. 199 (2001) 48.
[14] P. Mars, D.W. van Krevelen, Chem. Eng. Sci. Spec. Suppl. 3 (1954) 41.
[15] M.M. Schubert, S. Hacjenberg, A.C. van Veen, M. Muhler, V. Plzak, R.J. Behm, J. Catal. 197 (2001) 113.
[16] A. Sárkány, Z. Zsoldos, J.W. Hightower, L. Guczi, Catalytic Science and Technology, Kodansha, Tokyo, 1995, p. 99.